Event-triggered Consensus Control Approach for Guaranteed Finite Time Convergence – *Progress Report*

Liam Dale[1], n9741283
Dr. Aaron McFadyen[2]

***Abstract* – This document outlines the initial stages of an investigation into event-triggered consensus of multi agent systems guaranteeing finite time convergence. Based on a literature review basic state-dependent and state-independent triggering protocols are simulated. These conserve system resources while having satisfactory performance. They are augmented with open loop estimation techniques to improve effectiveness. A sky-highway use case is defined in the context of urban air mobility. Improvements considering practicality and robustness are planned for future work.**

I. Project Introduction

A century of aerospace innovation is culminating to the development of urban air mobility (UAM), which constitutes fully automated vertical take-off and landing aircraft (VTOL) for intra-city transportation [1]. When compared to road transport this technology may alleviate congestion and decrease travel time while faring at par or better regarding fuel costs and carbon dioxide emissions [2]. This has piqued interest from many entities including Uber and Airbus, which are already rolling out services on a small scale [3, 4]. Due to its infancy there are still many open questions regarding regulations and technical implementations [5].

Successful UAM realisation will see an increase in vehicle density along major aerial routes and highways which will eclipse the capability of contemporary air traffic management (ATM) systems. Thus, a challenge is posed to provide technologies which autonomously maintain safety and efficiency for dense multi-agent systems (MASs) with networking capabilities [1]. This will require all agents coordinate to observe a collective behaviour.

This project will focus on the topic of consensus, which typically refers to the problem of reaching an agreement among a group despite their initial state trajectories [6]. This is an integral component of group decision making and motion coordination. A typical example is platooning on highways, where vehicles negotiate a collective speed and heading to maintain a safe separation [6]. This project report focusses on decentralised event-triggered consensus as this has practical implications relevant to UAM.

This report details progress, and is structured as follows. Section II provides a background and literature review to further introduce the topic. Findings inform the research problem, which is outlined within section III. A design goal to contextualise the project is proposed in section IV which progress examples in section V are working towards. This all starts to come together in VI with the incorporation of nonlinear control. Finally, avenues for future work and a timeline for completion is detailed.

II. Background/Literature Review

Information sharing between MAS participants is essential for consensus such they may all agree on a common goal [6]. It may occur in a centralised manner, which assumes all agents communicate global knowledge over a fully connected network and solve the problem with a central node. This approach introduces a single point of failure and as communication topologies are rarely fully connected becomes increasingly impractical as the number of agents scales [7]. Alternatively there is a decentralised scheme, where information may only be shared between neighbours and nodes perform individual decision making. This method is pragmatic by virtues of robustness and scalability, however is more complex in structure and organisation [7].

Continuous communication between agents is unrealistic for practical applications, as it is an unnecessary drain on limited resources [8]. Alongside corresponding computation and actuator updates it consumes energy to drain batteries and curtail flight time. Networks constraints such as packet loss, latency and throughput worsen with congestion, endangering performance and stability [8]. Drawbacks are exacerbated as the network size scales. As such, it is important to conservatively transmit information while preserving the overall system performance [9]. Event triggered control is a solution where transmissions are spread sporadically based on current system measurements and an event-triggering threshold. This on-demand strategy significantly reduces transmission frequency while upholding performance [9].

While this investigation is tailored towards UAM the applications extend to networked control systems where resource conservation is important. Subterranean environments are critical to modern infrastructure. Due to harsh physical conditions and unforeseeable dangers such as fire or collapse it is preferable to use autonomous vehicles for many related operations [10]. A challenge is the limited communication infrastructure. In [10] autonomous mobile radio nodes traverse a collapsed mine to form a daisy chain and create an ad-hoc communications network. This enables tele-operated robots to clear rubble. An event-triggered

[1] **Liam Dale** is with Science and Engineering Faculty (SEF), Queensland University of Technology (QUT), Australia. This report is in partial fulfilment of EGH400-1 unit assessment requirements and submitted on 06-September-2020. liam.dale@connect.qut.edu.au.

[2] **Dr. Aaron McFadyen** is also with Science and Engineering Faculty (SEF), Queensland University of Technology (QUT), Australia. He is the supervisor for this research project.

solution would crucially extend node lifetime and preserve network resources.

A. Multi-Agent Consensus

The network topology plays an integral role in the consensus of a multi-agent system. It determines the rate of convergence, negotiated result and whether consensus is possible [6]. The topology is not necessarily fixed, being affected by vehicle motion and communication dropouts. Suppose there are n agents where the communication topology is modelled by a directed graph $G_n \triangleq (V_n, E_n)$. $V_n = \{1, 2 \dots n\}$ is the set of vertices and $E_n \subseteq V_n \times V_n$ is the set of edges. This system must have negotiations arbitrated by a consensus algorithm.

The most prevalent continuous-time consensus algorithm [6] is given as

$$\dot{x}_i(t) = -\sum_{j=1}^{n} a_{ij}(t)\left[x_i(t) - x_j(t)\right], \qquad i = 1, \dots, n$$

where $a_{ij}(t)$ is an entry in the associated adjacency matrix. Variables i and j respectively denote receiving and transmitting agents. State x denotes the information state, which relates to the consensus variable of interest. The corresponding matrix form is

$$\dot{x}_i(t) = -L_n(t)x(t)$$

where $L_n(t)$ corresponds to the G_n associated Laplacian matrix. Consensus is achieved when for each initial state $x_i(0)$ and for all $i, j = 1, \dots, n$ the difference of states $\left|x_i(t) - x_j(t)\right| \to 0$ as $t \to \infty$.

The continuous time algorithm is discretised with a difference equation [6]

$$x_i[k+1] = \sum_{j=1}^{n} d_{ij}[k]x_j[k], \qquad i = 1, \dots, n$$

where $d_{ij}[k]$ is an entry in the associated row-stochastic matrix D, and k denotes a sampling event. Information states are held constant between triggers. The corresponding matrix form is

$$x[k+1] = D[k]x[k]$$

Similarly, consensus is achieved when for each initial state $x_i[0]$ and for all $i, j = 1, \dots, n$ the difference of states $\left|x_i[k] - x_j[k]\right| \to 0$ as $k \to \infty$.

For both continuous and discrete time with invariant topologies and constant a_{ij} gains consensus is achieved when the directed topology has a directed spanning tree, or the undirected topology is connected. In these scenarios the Laplacian matrix eigenvalues $\lambda_i(L_p)$ are positive semidefinite, starting from zero and increasing. As such, non-zero eigenvalues $\lambda_i(-L_p)$ are all negative. The second smallest $\lambda_2(L_p)$ is the algebraic connectivity and defines the asymptotic convergence rate [6].

These algorithms force x_i to be driven towards the information state of its neighbours. Equilibrium is determined by vehicles which are the root of a directed spanning tree, equal to a weighted average of their initial states [6]. This property gives rise to leaderless, and leader-follower strategies. When there is a single leader it becomes a reference for all followers, which is often the case in platooning. For leaderless networks if a reference is desired an intangible virtual leader may be created to emulate this behaviour [6]. For undirected connected graphs all nodes are leaders and followers giving average consensus [6].

With controllers being connected over a network, the consensus should be robust to wireless channel constraints and stochasticity [7]. Issues such as fading, variable latency, packet misses and quantisation cause the system and controller inputs to be an approximation of measured values. These issues have the potential to degrade performance and stability [7], and alongside network topology changes are not addressed in the general algorithm mentioned.

B. Consensus for Single-Integrator Dynamics

Consider agents where the information state dynamics are given as the control input [6].

$$\dot{\xi}(t) = u_i(t), \qquad i = 1, \dots, n$$

The fundamental consensus algorithms are then altered as follows

$$\mathrm{u_i(t)} = -\sum_{j=1}^{n} a_{ij}(t)\left[\xi_\mathrm{i}(t) - \xi_j(t)\right], \qquad i = 1, \dots, n$$

$$\xi_i[k+1] = \sum_{j=1}^{n} d_{ij}[k]\xi_j[k], \qquad i = 1, \dots, n$$

and in matrix forms

$$\dot{\xi} = -|L_n(t) \otimes I_m|\xi$$
$$\xi[k+1] = -|D_n[k] \otimes I_m|\xi[k]$$

where $\otimes$ denotes the Kronecker product. The concepts for stability and convergence are analogous to before.

This algorithm may be extended to guarantee that information states converge to a set difference Δ_{ij}, such that

$$(\xi_\mathrm{i} - \xi_j) \to \Delta_{ij}(t) \text{ as } t \to \infty \text{ [6].}$$

$$\mathrm{u_i(t)} = \dot{\delta}_i - \sum_{j=1}^{n} a_{ij}\left[(\xi_\mathrm{i} - \xi_j) - (\delta_i - \delta_j)\right], \qquad i = 1, \dots, n$$

Here $\Delta_{ij} \triangleq \delta_i - \delta_j, \forall i \neq j$ where δ describes the relative state reference of the corresponding agent. This algorithm is useful for maintaining relative vehicle positions, which has applications in formation control.

C. Event-Triggered Consensus Protocols

For resource conservation communications and corresponding actuator updates may be spread over discrete time intervals, between which measured values are locked and held. There must be a sufficient frequency to effectively capture state changes and preserve performance goals. Conversely there must be a guaranteed lower bound on inter-event execution times to exclude Zeno behaviour, where infinite events happen on a finite time horizon [11].

The sampled-data approach is where transmissions are delayed by a fixed period, although improving utilisation this still results in an over-provisioning of resources. High frequency triggers required to maintain stability and provide new information in the transient phase are excessive as the system converges [11]. A dynamic approach is required to overcome this limitation.

An event-triggered protocol transmits information on demand to reduce wastage without jeopardising performance.

A core component is the error measurement e between the current states x and latest broadcast states $\hat{x}$

$$\hat{x}_i(t) = x_i(t_k^i), \qquad t \in [t_k^i, t_{k+1}^i)$$
$$e(t) = \hat{x}(t) - x(t)$$

where $t_0^i, t_1^i, \ldots$ are the triggering instants for agent i. This provides a measure on how valuable the state of an agent is to maintaining overall closed loop behaviour. Events are triggered when this crosses a dynamic threshold e_T and so at all times the following condition holds.

$$error \leq threshold \triangleq e(t) \leq e_T(t)$$

On triggering agents broadcast their states and alongside receivers update their control inputs accordingly. As controllers use periodically broadcast values the input is redefined as

$$\mathrm{u_i(t)} = -\mathrm{K}\sum_{j=1}^{n} a_{ij}(t)\left[\hat{x}_i(t) - \hat{x}_j(t)\right], \qquad i = 1, \ldots, n$$

where K is a gain matrix and again agent i receives from agent j. A basic operating procedure is represented in Figure 1 below. The error threshold is selected to preserve underlying consensus stability concepts such as Lyapunov stability, input-to-state stability (ISS) and L_2 stability. The latter two are preferred in practical systems due to their robustness against external disturbances.

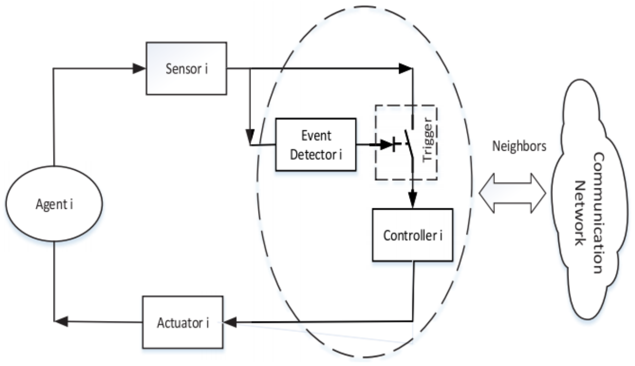

Figure 1 Event Triggering Process [11]

An early event triggered consensus strategy for a linear multi-agent system of N agents is considered in [12] for undirected, connected topologies. The solution is extensible to high order dynamics, described via

$$\dot{x}_i(t) = Ax_i(t) + Bu_i(t), \qquad i = 1,2, \ldots N$$

assuming

$$rank(AB) = rank(A)$$

It is also robust to switching topologies, and enforces a lower boundary on the inter-execution time to exclude Zeno behaviour for all agents. The event triggering-threshold given as

$$e_T(t) = k_i|z_i(t)|, i = 1,2, \ldots N$$

where

$$0 < k_i < 1/\max\,(\lambda_N[L_p(t)])$$
$$z_i(t) = \textstyle\sum_{j=1}^{N} a_i(x_i(t) - x_j(t))$$

This relaxes the actuation update requirements, however $z_i(t)$ still requires constant knowledge of neighbouring states and global topology – contradicting motivations and leaving continuous communication as a requirement. Communication is relaxed in [13] to use only broadcasted states at the expense of a more complex triggering function. Assumptions of linearity and an undirected topology simplify event triggering, however, raise practical concerns.

An alternative strategy using a state-independent threshold for relative error is proposed in [14] for an undirected, connected topology. The triggering threshold is given as

$$e_T(t) = c_0 + c_1 e^{-\alpha t}$$

with constants

$$c_0 \geq 0, c_1 \geq 0, c_0 + c_1 > 0$$
$$0 < \alpha < \lambda_2(L_p)$$

By only needing local information to compute the state-triggering condition the need for continuous communication is eliminated. Design choices are required for c_0, c_1 and α. If the choice for $c_0 \neq 0$ then consensus is not exact but bounded by a radius but Zeno behaviour is automatically excluded. Details are also given on extensions to accommodate for network stochasticity and double-integrator agents. The assumptions of linear dynamics and network topologies are again impractical.

These strategies will continue to trigger when consensus is reached unless agents are at an equilibrium point. The error thresholds trend towards zero as either the agents converge or time elapses. When they are arbitrarily small if any agent deviates from its latest broadcast value the error is enough to trigger an event [15]. These triggers are not crucial to maintaining consensus, and so are a contradictory wastage of resources. In many autonomous vehicle scenarios this is a hard limitation as agents are constantly moving.

D. *Model-Based Event-Triggered Consensus Protocols*

Model-based event-triggered control protocols employ observer estimation techniques to the predict error and reduce triggering frequency [16]. There is a computational cost as agents must be equipped with estimators for themselves and each of their leaders. If the network is not homogenous agents must also communicate their dynamics. As the network scales these burdens grow [15]. There are open loop and closed loop estimation techniques.

In the open loop estimation approach the latest broadcasts are projected forwards without control inputs. They may be rewritten as

$$\hat{x}_i(t) = e^{A(t-t_k^i)}x_i(t_k^i), \qquad t \in [t_k^i, t_{k+1}^i)$$

where A is a linear state dynamics matrix for agent i. This redefines the control input and error [16]

$$\mathrm{u_i(t)} = -\mathrm{K}\sum_{j=1}^{n} a_{ij}(t)\left[e^{A_i(t-t_k^i)}x_i(t_k^i) - e^{A_j(t-t_k^j)}x_j(t_{k'}^j)\right]$$
$$e_i(t) = e^{A(t-t_k^i)}x(t_k^i) - x(t)$$

where $t_{k'}^j$ denotes a triggering instant for agent j. State dependent and independent protocols utilising this technique are studied in [16] and [17] respectively.

A discretised version of this technique is presented in [17]. The estimation is given recursively from the latest broadcast as

$$\hat{x}_i[k] = G^{(k-k_q^i)} x_i[k_q^i], \qquad k \in \left[k_q^i, k_{q+1}^i\right)$$

where G is the discrete state space dynamics matrix and k_q^i denotes triggering iterations of agent i. The event threshold is taken as

$$e_T(k) = c\alpha^{kT}$$

with T as the discrete time step and the following constants.

$$c > 0$$

$$\max(|\lambda(\Xi)|) < \alpha < 1$$

For N agent states and n network agents matrix $\Xi \in \mathbb{C}^{(n-1)N \times (n-1)N}$ is given as

$$\Xi \triangleq I_{n-1} \otimes G + \Delta \otimes HK$$

where H is the discrete time input matrix and I is an identity matrix. Finally, $\Delta \in \mathbb{C}^{(n-1)\times(n-1)}$ is the submatrix of the Jordan canonical form of $I_n - D_{in}$ without row and column one. D_{in} is the topology in-degree matrix (see Appendix I matrix preliminaries). Compared to the previously surveyed state-dependent protocol this threshold requires more calculation. An advantage is that agent dynamics are considered. Discrete sampling inherently provides a lower boundary on inter-event times to exclude Zeno behaviour and so there is no bounding constant needed. Perfect consensus is enforced.

The closed loop approach makes estimates with a control input. It follows that agents must additionally broadcast their inputs on event triggers. This requires drastic alteration of the generic strategy; if $\hat{x}$ reflects the measured states there is no error to trigger. The strategy is considered in [18] where agents are triggered by virtual edge systems which consider the difference in states and inputs of their two vertices. Advantages are only seen in the transient phase. When consensus is reached control inputs are zero, and this technique becomes analogous to the open loop estimation. Input broadcasting merits further review and consideration. If agents can estimate the states of their neighbours the continuous monitoring requirements of protocols surveyed in the previous subsection are relaxed.

E. *Finite Time Convergence*

The convergence rate is a significant performance metric for consensus control, so a typical problem is to develop controllers which drive the system in as little time as possible [6]. Most control schemes use Lipschitzian dynamics, leading to exponential convergence with infinite settling time [19] and dependence on initial state conditions [11]. With an event-triggering protocol which aims to reduce control updates, this may suffer further [11]. This motivates practical MAS design to reach consensus in finite time. Research in this area is attracting attention and evolving rapidly, with recent approaches in [20, 21, 22, 23].

An early event-triggered finite time consensus control scheme is proposed in [24] for a mobile sensor network. This designs a finite-time consensus algorithm and determines a state-dependent event-triggering rule to preserve stability. The triggering condition has increased complexity, and still requires continuous communication. Results show that when compared to a standard benchmark performance is maintained while reducing computational resource usage and control updates.

F. *Nonlinear Control*

Most physical systems are governed by nonlinear dynamics. For a practical UAM implementation nonlinear control techniques must be studied.

1. Gain Scheduling

Gain scheduling is an adaptive control technique where controller parameters change with the plant operating conditions [25]. The high level architecture is pictured in Figure 2. A primitive version was introduced for missile guidance where feedforward gain would adjust to compensate for the varying effects of air pressure and Mach number [25]. This is particularly salient for an event-triggered design as the adaptation is minimised. Similarly, with distributed computing this is feasible for a MAS.

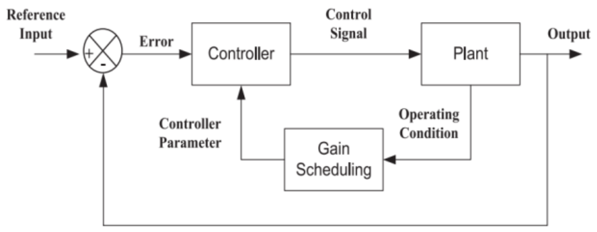

Figure 2 Gain Scheduling Architecture [26]

The design of a gain scheduled controller can be generalised to a three-step process [25]. The first is to select a set of operating points covering the plant range. System values and nonlinearities are formulated as time-varying parameters. Following this a linear approximation is constructed for each point, and an appropriate controller is designed. Finally, gains are interpolated to ensure smooth transitions and create a global compensator. During operations the calculated gains are decided with real-time measurements.

III. Research Problem

The aim of this project is to investigate a practical approach for a MAS to achieve consensus. As a foundational concept in unmanned traffic management (UTM) this is quintessential for the successful realisation of future UAM.

This research will simulate average consensus amongst homogeneous agents under an undirected network. Communication will be event triggered and guarantee convergence within finite time to achieve a balance of feasibility and performance. This will lay the foundation to explore robustness.

Even minor disturbances can greatly affect the event-triggering performance and consensus. When the triggering threshold is low they can cause unnecessary events and undercut design goals. Alternatively with bounded consensus and sporadic triggers the system precision is reduced.

Network artefacts such as transmission latency, dropouts and quantisation are also relevant to large MASs. They will not be considered within this paper however as their effects are abated by avoiding continuous communication. This reiterates the importance of minimising unnecessary disturbance related events.

IV. Design Program

Working towards a practical implementation requires that a realistic scenario be modelled. This section details some practical considerations towards the final outcome.

A. Vehicle Dynamics

Two nonlinear vehicle models are defined within this subsection. They are similar, although have different physical states and levels of actuation.

These models may be linearized to enable to the use of simple linear control techniques. This requires calculation of the Jacobian state and input matrices (see Appendix I.C). These are denoted respectively as $A(\bar{\boldsymbol{x}},\bar{\boldsymbol{u}})$ and $B(\bar{\boldsymbol{x}},\bar{\boldsymbol{u}})$, where $\bar{\boldsymbol{x}}$ and $\bar{\boldsymbol{u}}$ are state and input vectors which linearization has occurred around. These may be calculated at different operating points, provided that the system is measured or completely observable.

The nonlinear model may be approximated in the state space form as follows.

$$\dot{\boldsymbol{x}} = A(\bar{\boldsymbol{x}},\bar{\boldsymbol{u}})\boldsymbol{x} + B(\bar{\boldsymbol{x}},\bar{\boldsymbol{u}})\boldsymbol{u}$$

The approximation will worsen as the actual points diverge from $\bar{\boldsymbol{x}}$ and $\bar{\boldsymbol{u}}$. An inherent limitation of the representation accuracy is the discrete time sampling interval.

1. Quadrotor

The idealised rigid-body dynamics of a quadrotor vehicle [27] are a candidate to contextualise this project within UAM. There are three degrees of freedom with cartesian x-y motion and rotation about a single axis. These are controlled by front and rear actuator forces F_F and F_R. This can be seen below in Figure 3. States considered are x position, x momentum, y position, y momentum, pitch angle, and angular inertia. These are as follows.

$$\boldsymbol{z_1} \triangleq [x \quad p_x \quad y \quad p_y \quad \theta \quad L]^T$$
$$\boldsymbol{F_1} \triangleq [F_F \quad F_R]^T$$

The state derivatives are as follows.

$$\dot{\boldsymbol{z}}_{\boldsymbol{1}} = \begin{bmatrix} \dot{x} \\ \dot{p}_x \\ \dot{y} \\ \dot{p}_y \\ \dot{\theta} \\ \dot{L} \end{bmatrix} = \begin{bmatrix} \dot{z}_1 \\ \dot{z}_2 \\ \dot{z}_3 \\ \dot{z}_4 \\ \dot{z}_5 \\ \dot{z}_6 \end{bmatrix} = \begin{bmatrix} m^{-1}z_2 \\ -(F_F+F_R)\sin(z_5) \\ m^{-1}z_4 \\ (F_F+F_R)\cos(z_5) - mg \\ J^{-1}z_6 \\ l_F F_F - l_R F_R - b_t J^{-1} z_6 \end{bmatrix}$$

Table 1. Quadrotor Variable Descriptions

Variable	Description
m	Vehicle mass
g	Gravity constant
J	Moment of inertia around centre mass
b_t	Aero-dynamic damping
F_F, F_R	Thrust force of front rotors, rear rotors
l_F, l_R	Distance from centre mass of front rotor, rear rotor thrust vectors

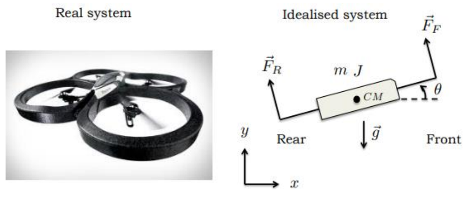

Figure 3 Quadrotor Model

The Jacobian matrices for this model are shown below.

$$A_1(\boldsymbol{z},\boldsymbol{F}) = \begin{bmatrix} 0 & m^{-1} & 0 & 0 & 0 & 0 \\ 0 & 0 & 0 & 0 & -(F_F+F_R)\cos(z_5) & 0 \\ 0 & 0 & 0 & m^{-1} & 0 & 0 \\ 0 & 0 & 0 & 0 & -(F_F+F_R)\sin(z_5) & 0 \\ 0 & 0 & 0 & 0 & 0 & J^{-1} \\ 0 & 0 & 0 & 0 & 0 & -b_t J^{-1} \end{bmatrix}$$

$$B_1(\boldsymbol{z},\boldsymbol{F}) = \begin{bmatrix} 0 & 0 \\ -\sin(z_5) & -\sin(z_5) \\ 0 & 0 \\ \cos(z_5) & \cos(z_5) \\ 0 & 0 \\ l_F & -l_R \end{bmatrix}$$

$$C_1 = \boldsymbol{I_6}, \qquad D_1 = \boldsymbol{0}^{\boldsymbol{6\times 2}}$$

2. Hovercraft

A hovercraft model may be used for this application [28]. It is very similar to the surveyed quadrotor. Again, there are three degrees of with x-y motion and single axis rotation. This system is more actuated, having starboard, port and lift actuators F_S, F_P and F_L. States considered are x momentum, x acceleration, y momentum, y acceleration, pitch angle and angular velocity. Figure 4 pictures this. These are represented as follows.

$$\boldsymbol{z_2} \triangleq [p_x \quad \dot{p}_x \quad p_y \quad \dot{p}_y \quad \theta \quad \dot{\theta}]^T$$
$$\boldsymbol{F_2} \triangleq [F_S \quad F_P \quad F_L]^T$$

The following details state derivatives.

$$\dot{\boldsymbol{z}}_{\boldsymbol{2}} = \begin{bmatrix} \dot{p}_x \\ \ddot{p}_x \\ \dot{p}_y \\ \ddot{p}_y \\ \dot{\theta} \\ \ddot{\theta} \end{bmatrix} = \begin{bmatrix} \dot{z}_1 \\ \dot{z}_2 \\ \dot{z}_3 \\ \dot{z}_4 \\ \dot{z}_5 \\ \dot{z}_6 \end{bmatrix} = \begin{bmatrix} z_2 \\ (F_s+F_P)\cos(z_5) - F_L\sin(z_5) - z_2 \\ z_4 \\ (F_s+F_P)\sin(z_5) + F_L\cos(z_5) - z_4 \\ z_6 \\ F_s - F_p - z_6 \end{bmatrix}$$

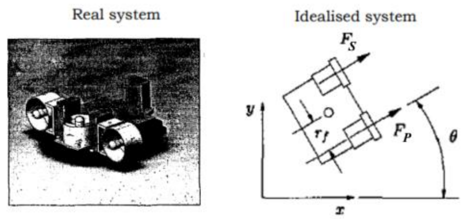

Figure 4 Hovercraft Model

For the purpose of linearisation, the Jacobian matrices are as follows.

$$A_2(\boldsymbol{z},\boldsymbol{F}) = \begin{bmatrix} 0 & 1 & 0 & 0 & 0 & 0 \\ 0 & -1 & 0 & 0 & -(F_s+F_p)\sin(z_5) - F_l\cos(z_5) & 0 \\ 0 & 0 & 0 & 1 & 0 & 0 \\ 0 & 0 & 0 & -1 & (F_s+F_p)\cos(z_5) - F_l\sin(z_5) & 0 \\ 0 & 0 & 0 & 0 & 0 & 1 \\ 0 & 0 & 0 & 0 & 0 & -1 \end{bmatrix}$$

$$B_2(\boldsymbol{z},\boldsymbol{F}) = \begin{bmatrix} 0 & 0 & 0 \\ \cos(z_5) & \cos(z_5) & -\sin(z_5) \\ 0 & 0 & 0 \\ \sin(z_5) & \sin(z_5) & \cos(z_5) \\ 0 & 0 & 0 \\ 1 & -1 & 0 \end{bmatrix}$$

$$C_2 = \boldsymbol{I}_6, \quad D_2 = \boldsymbol{0}^{6\times 3}$$

B. *Use Case*

Future UAM may be realised with a free flight style which is not governed by an organisational system [29]. Vehicles may be freely launched and compete for available airspace. They travel the shortest path to their destination and when anticipating collision employ sense and avoid technologies [29]. This will require minimal infrastructure to implement however presents significant safety challenges.

The air highway method of air traffic control provides a safer and more orderly alternative to free flight [29]. It emulates land freeways by geofencing air traffic paths for UAVs to follow. These are splits into directed lanes for travel, passing and damaged vehicles. Paths are carefully planned to preclude agents from crossing. With designated paths the route from source to destination is less efficient than free flight [29]. This idea has not been thoroughly tested or studied, so an optimal design is not known.

The project considers the air highway method of traffic control due to its safety merits. It models a sky highway separated into five lanes without speed limits. Using the cartesian XY plane lanes span the horizontal direction and are stacked vertically. Agents in each lane communicate with their two adjacent neighbours. They aim to reach a consensus on horizontal velocity while specifying a dynamic formation with minimum offsets avoid loss of separation. New agents are periodically spawned around the entry point with random initial conditions and merge into their closest lane. This causes the network topology to switch. Lane boundaries are predefined so agents do not need to use consensus techniques to negotiate the vertical position or velocity.

A preliminary simulation has been performed. Dynamics are those as discussed in section V, however these are extended with another actuator and independent dimension. A model-based state-dependent triggering strategy also discussed in V is used. Updates to actuators are coupled, however with the simplified dynamics they could be separated. Vertical position and velocity are not decided via consensus and so should be triggered independently of network status. The exact triggering mechanisms will be subject to change when dynamics are update and the use case evolves. A demonstrative animation is available for viewing at https://github.com/ldale1/EGH400-Event-Triggered-Consensus/tree/master/Animations.

C. *Disturbance Rejection*

Aerial vehicles are susceptible to the effects of wind and other environmental conditions. This is especially pertinent for small UAVs, which may be blow off course and risk collision [29]. A wind model will be applied to agents to verify their robustness against exogenous disturbances. This will take the form of the U.S. Naval Research Laboratory Horizontal Wind Model, which is available through MATLAB [30]. The chosen simulation location is Brisbane city.

The application of the wind model will be simple. Causing acceleration it will singularly affect the momentum rate of change. Changes to pitch will not be considered despite the practical implications. Applied force F_W is calculated proportionally to the relative system speed as follows [31].

$$F_W = C(v_{SYS} - v_w)^2$$

Here v_{SYS} and v_w respectively denote the agent and wind velocities. C is an aggregation of constants such as the drag coefficient, effective aperture and fluid density. In the state space this may be modelled as a disturbance.

D. *Operating Regime*

For each agent their operations are simulated with the following algorithm in discrete time. Samples t_k are synchronised for all agents, however this may not be the case in practice.

Algorithm 1. Network Simulation

```
01:  $t_k \leftarrow 0$
02:  $\hat{x} \leftarrow x_0$
03:  Broadcast $\hat{x}$
04:  While $t_k < t_{sim}$
       Check for transmissions
05:    If (receiving transmission from any leader $j$)
06:      $\hat{x}_j \leftarrow x_j$
07:      Recalculate control input $u$
08:    End if
       Check for an event
09:    If ($\|e\| > \|e_T\|$)
10:      $\hat{x} \leftarrow x$
11:      Broadcast $\hat{x}$
12:      Recalculate control input $u$
13:    End if
       Decide on control input
14:    If (recalculated control input)
15:      Update actuator
16:    Else
17:      Hold actuator
18:    End if
       Ready for the next sample
19:    Step agent
20:    If (model-based protocol)
21:      Project states $\hat{x}$
22:      Project leader states $\hat{x}_j$
23:    End if
24:    $t_k \leftarrow t_{k+1}$
25:  End while
```

This models a time-invariant topology. When this switches the new topology is modelled as a contiguous scenario. The algorithm restarts with the initial states as the final states of the previous topology.

V. Consensus Algorithm Exploration

Consider a strongly connected network with five agents. They have simple linear dynamics described as follows.

$$\dot{x}_i = \begin{bmatrix} 0 & 1 \\ 0 & 0 \end{bmatrix} x_i + \begin{bmatrix} 0 \\ 1 \end{bmatrix} u_i$$

where x_i and u_i denote states and control input for agent i. The Laplacian communications matrix and associated eigenvalues λ_L are as follows.

$$L = \begin{bmatrix} 4 & -1 & -1 & -1 & -1 \\ -1 & 4 & -1 & -1 & -1 \\ -1 & -1 & 4 & -1 & -1 \\ -1 & -1 & -1 & 4 & -1 \\ -1 & -1 & -1 & -1 & 4 \end{bmatrix}$$

$$\lambda_L = [0, 5, 5, 5, 5]$$

The system is modelled in discrete time, with a sampling period of 0.01 seconds. The corresponding discrete time dynamics are given as follows.

$$x_i[k+1] = \begin{bmatrix} 1 & 0.01 \\ 0 & 1 \end{bmatrix} x_i[k] + \begin{bmatrix} 0.0001 \\ 0.01 \end{bmatrix} u_i[k]$$

The row-stochastic communications matrix and associated eigenvalues λ_D are given below.

$$D = \begin{bmatrix} 0.2 & 0.2 & 0.2 & 0.2 & 0.2 \\ 0.2 & 0.2 & 0.2 & 0.2 & 0.2 \\ 0.2 & 0.2 & 0.2 & 0.2 & 0.2 \\ 0.2 & 0.2 & 0.2 & 0.2 & 0.2 \\ 0.2 & 0.2 & 0.2 & 0.2 & 0.2 \end{bmatrix}$$

$$\lambda_D = [0, 0, 0, 0, 1]$$

Initial state values are given as $x_1(0) = [5.5; 9.5]$, $x_2(0) = [-4.5; -6.5]$, $x_3(0) = [12.5; -0.5], x_4(0) = [9.5; -1.5]$ and $x_5(0) = [-0.5; 2.5]$. Their controller gains are $K = [0.99, 1.72]$ as decided by a discrete linear quadratic regulator which penalises states and inputs equally.

A. State-Dependent Event Trigger

Using the state-dependent event trigger in [12] adapted for discrete time agent trajectories are pictured as follows. Consensus is successfully reached. The settling value for state two is 0.7, which is the average of initial values.

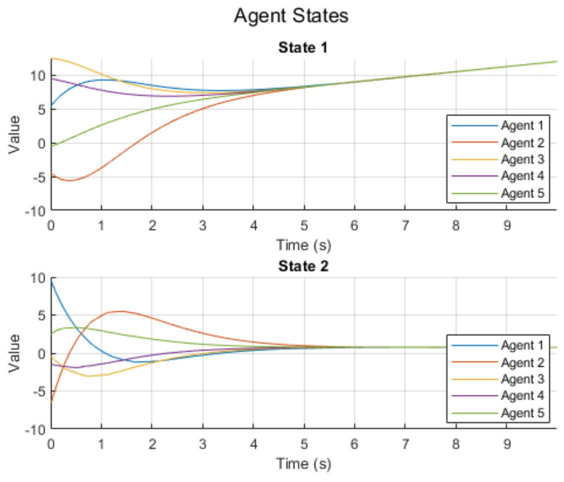

Figure 5 Scenario V.A State Trajectories

During the transient phase triggering instants observe intended behaviour. Agents one and two have the largest initial velocities. Their rapid movement causes frequent early triggers. As they adjust their speed this frequency reduces. When agents near consensus their triggering frequency increases rapidly, contradicting design goals. On average 40.7% of samples are triggered. Actuator updates are more common as they also relate to neighbour transmissions. This ratio will worsen as time draws out due to extreme steady state triggers.

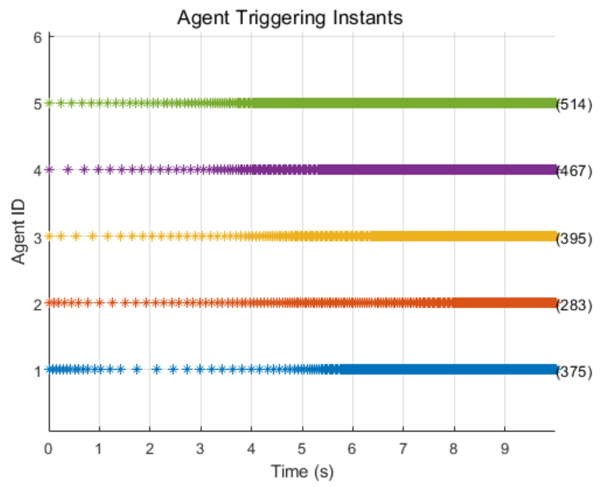

Figure 6 Scenario V.A Triggering Instants

Rapid triggering as consensus is approached is mirrored by an arbitrarily small error threshold. As state two settles on a nonzero value state one will always be drifting from its latest broadcast. Without a predictive factor the error grows and consistently triggers events. State one cannot be overlooked in triggering as it could be used to dictate the MAS formation. Magnitude of state two corresponds to steady state triggering frequency.

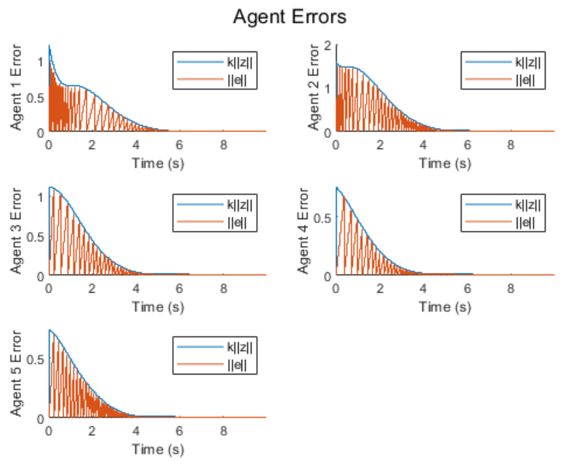

Figure 7 Scenario V.A Error and Threshold Norms

B. Model-Based State Dependent Event Trigger

This scenario uses the same event trigger, however predicts error with an open loop estimation approach. State trajectories and differences to the previous scenario are pictured below. Despite transient differences agents settle at the same states.

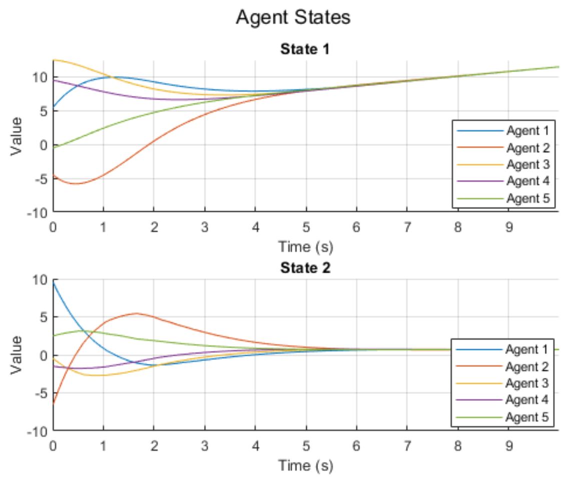

Figure 8 Scenario VIII.BV.B State Trajectories

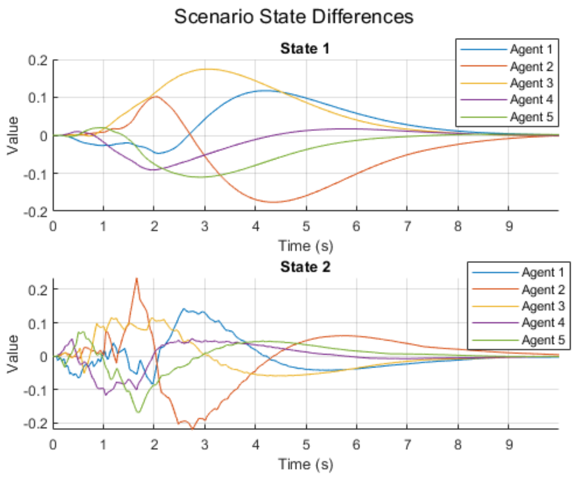

Figure 9 Scenario V.A and V.B State Differences

With the predictive factor agents stops triggering when consensus is reached. Net triggering has been reduced to 4.9% of all samples to better align with the intent. This ratio will improve as time draws out and the network is undisturbed.

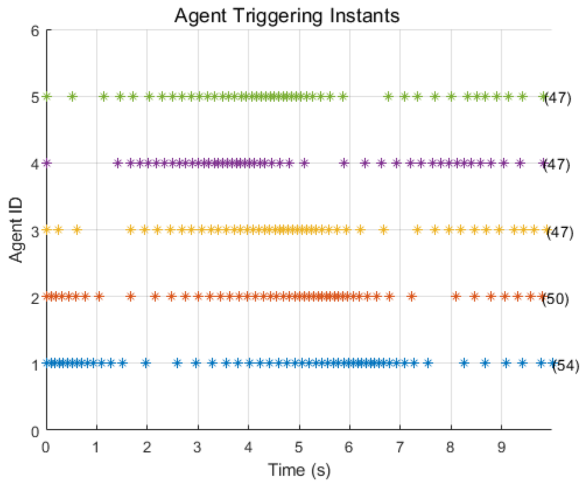

Figure 10 Scenario V.B Triggering Instants

C. Model-Based State Dependent Event Trigger under Switching Topologies

This scenario models a network which switches to a randomly generated, undirected topology every second. No restrictions are placed on their layout. The progression is shown in the succeeding figure.

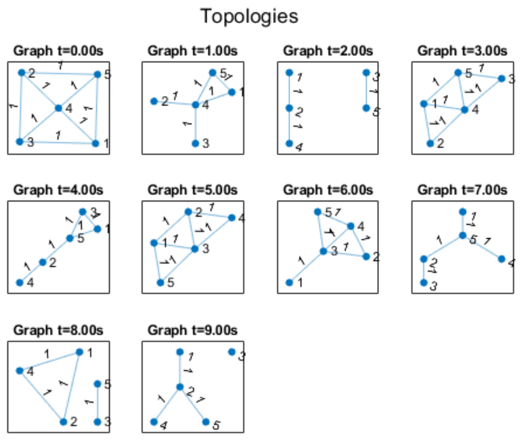

Figure 11 Scenario V.C Topology Progression

Agents and protocol are the same as in scenario V.B. Simulated trajectories are shown in the figure below. These have become jagged, as agent constantly switch leaders. When completely disconnected agents have zero control input and state two stays unchanged. Consensus is still achieved as with enough random changes agents inevitably transmit states across the network. As switching frequency increases the result becomes more analogous to the previous scenario. Settling has been drawn out, and the final state two value has dropped 17.1% to a value of 0.58.

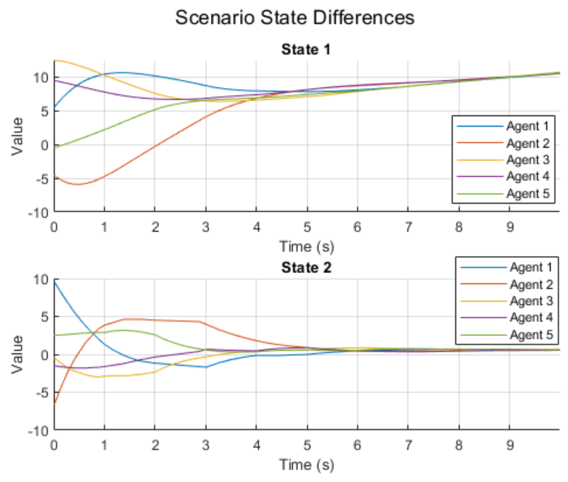

Figure 12 Scenario V.C State Trajectories

Topology changes trigger an event. Whether events keep triggering depends on state derivatives and updated error thresholds. When thresholds quickly drop agents adjust rapidly with frequent triggers.

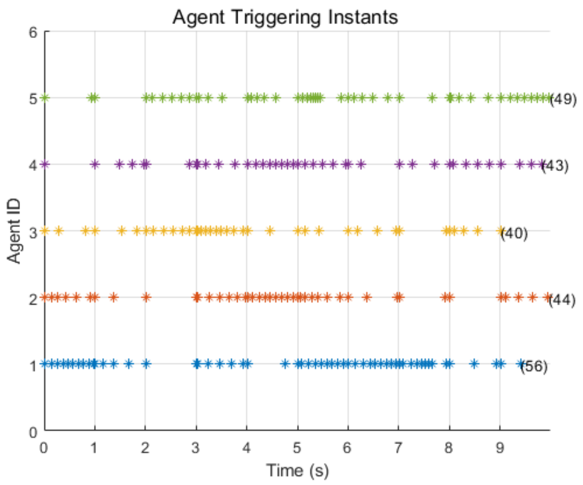

Figure 13 Scenario V.C Triggering Instants

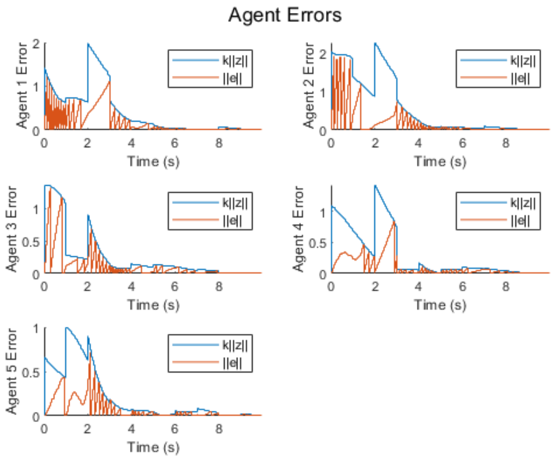

Figure 14 V.C Scenario Error and Threshold Norms

When there is a topology switch agent control inputs can change quite drastically. This is especially relevant when an agent suddenly becomes led by a single neighbour with different states. A mild example is seen in the succeeding figure at two seconds. A practical worry may be actuator switching speed and saturation.

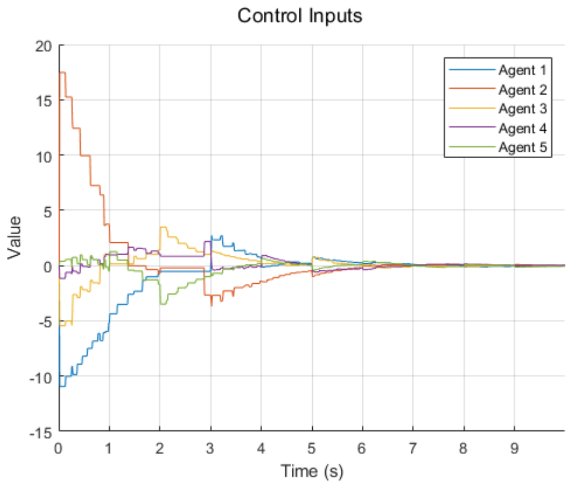

Figure 15 Scenario V.C Control Inputs

D. *Model-Based State-Independent Event-Trigger*

This scenario implements the model-based state-independent protocol surveyed in II.D with an invariant strongly connected topology. Constant c is chosen as 0.5 arbitrarily. The eigenvalues of matrix Ξ are all $0.9913 \pm 0.05i$ giving constant α as 0.992. State trajectories are similar to previous scenarios.

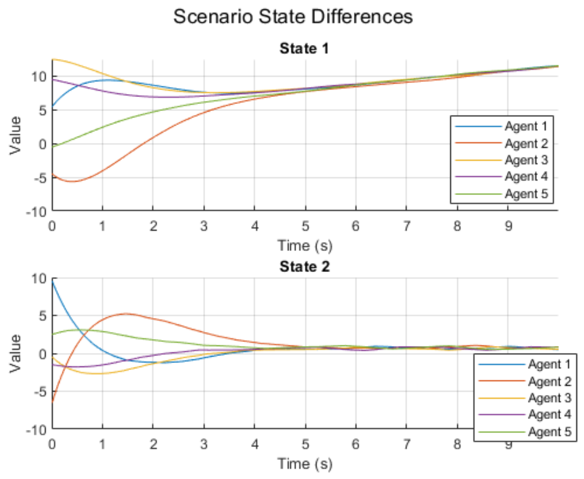

Figure 16 Scenario V.D State Trajectories

Event triggers are very infrequent as shown in the figure overleaf. As a consequence agents are not pushed to a precise consensus speedily; there is still a spread at ten seconds. This is reflected by the error threshold, which decays slowly uninfluenced by neighbours. Empirically the rate for perfect convergence is an inherent challenge for state-independent thresholds. While this may be affected by design choices if the exponential term decays too quickly the threshold goes to zero and appears as a fixed trigger. Given topology switches the threshold does not adapt.

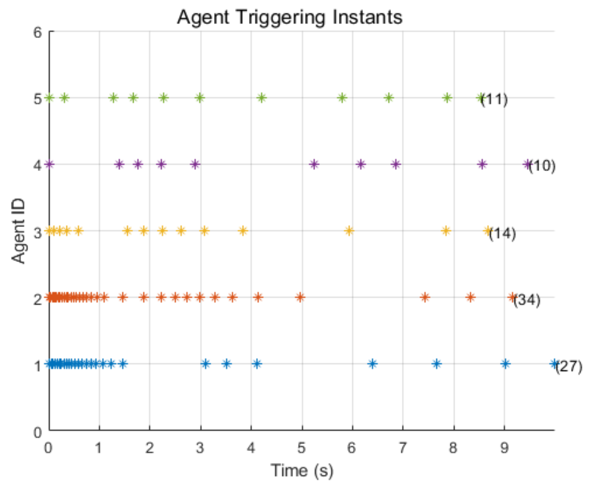

Figure 17 Scenario V.D Triggering Instants

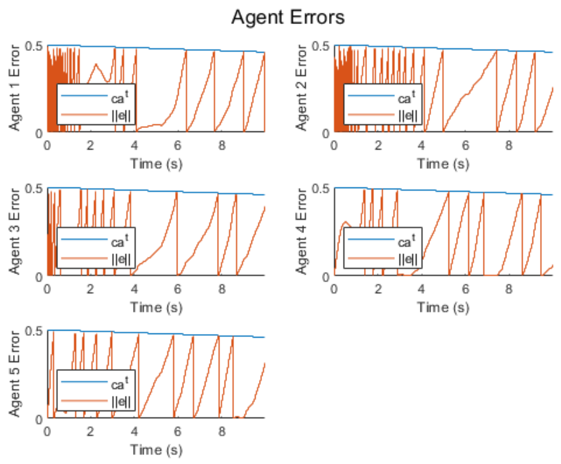

Figure 18 Scenario V.D Error and Threshold Norms

VI. Non-Linear Control

For practical UAM nonlinear control techniques must be employed. This section investigates the efficacy of surveyed approaches using described quadrotor and hovercraft dynamical models. The model-based state dependent triggering rule is employed. The following scenarios are used as demonstrations.

Scenario One:

Consider a strongly connected network of three hovercrafts. They start with the initial conditions as follows, and the discrete sampling time is 0.01 seconds. The control objective is to reach consensus on all states.

$$x_{01} = [5 \quad 1 \quad -8 \quad -3 \quad 3\pi/8 \quad -1]^T$$
$$x_{02} = [1 \quad -6 \quad 2 \quad 5 \quad \pi/8 \quad -1]^T$$
$$x_{03} = [-13 \quad -0.2 \quad 4 \quad -1 \quad \pi/24 \quad 1]^T$$

Scenario Two:

Consider the same network described in scenario one. The initial conditions are altered as follows. Most notably the angular velocity (state six) magnitudes have been increased. This is designed to test stability.

$$x_{01} = [5 \quad 1 \quad -8 \quad -3 \quad 3\pi/8 \quad -5]^T$$
$$x_{02} = [1 \quad -6 \quad 2 \quad 5 \quad \pi/8 \quad -3]^T$$
$$x_{03} = [-13 \quad -0.2 \quad 4 \quad -1 \quad \pi/24 \quad 3]^T$$

A. Linearisation

A fixed gain linear controller is designed as a baseline performance benchmark. For this the following operating point is selected.

$$\bar{x} = [0 \quad 0 \quad 0 \quad 0 \quad \pi/4 \quad 0]^T$$
$$\bar{u} = [0\ 0\ 0]^T;$$

This was chosen to reflect zero to ninety degree range where the initial states in both scenarios lie. Throughout this span in-phase cos and sin terms both have consistent signs. This is relevant as it reflects overall direction in the dynamical model. The initial states in both scenarios lie within this area. The combination of these two factors ideally maximises the valid controller range.

The get the gain values a linear quadratic regulator is used. This is performed in MATLAB with the Jacobian matrices calculated at $\bar{x}, \bar{u}$. States and inputs are penalised equally to give the following gain matrix.

$$K = \begin{bmatrix} 0.5 & 0.5 & 0.5 & 0.5 & \sqrt{2} & \sqrt{2} \\ 0.5 & 0.5 & 0.5 & 0.5 & -\sqrt{2} & -\sqrt{2} \\ -\sqrt{2} & -\sqrt{2} & \sqrt{2} & \sqrt{2} & 0 & 0 \end{bmatrix}$$

The resultant control law is $u = -Kx$.

The scenario one simulation is successfully stabilised. The state trajectories can be seen below. Pitch angle (state five) remains between the designed controller range for each agent. Event triggers are infrequent, occurring 51 times within 3000 total discrete sampling instants.

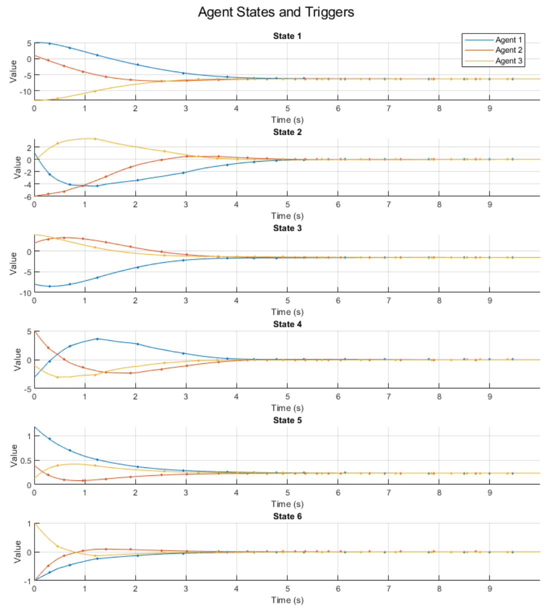

Figure 19 Fixed Controller Scenario 1

The scenario two simulation has not been stabilised. State trajectories are pictured in Figure 20. Noticeably the large initial angular velocities cause rotational overshoot, and the pitch angle is driven negative outside the desired range. Without an updated assessment on how inputs are affecting agents the controller cannot regulate the system.

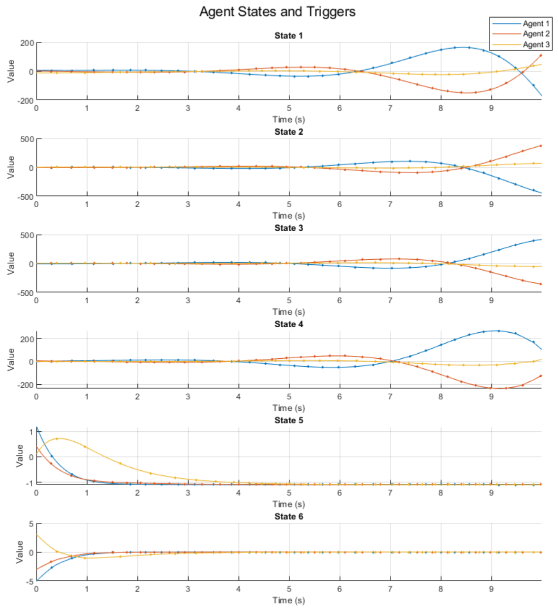

Figure 20 Fixed Controller Scenario 2

B. *Gain Scheduling*

Gains for a simple feedback controller may be scheduled to increase the stability region. To perform this the system is linearised at its current operating point when an event is triggered or received. A linear quadratic regulator penalising states and inputs equally calculates the gain for stability. This updated controller design is accurate until the states diverge, at which new gains are ushered in through an event trigger.

Scenario one is again successfully stabilised. State trajectories are pictured in the succeeding figure. The final values are now different, however the settling times are similar. In the leading transient phase trajectories are not as smooth. This is a function of event triggers causing a discontinuous jump in control input coupled with a change in the gain. Fluctuations are seen most aggressively for the pitch angle. Event triggers have been trimmed 35% to be 33 of 3000 samples.

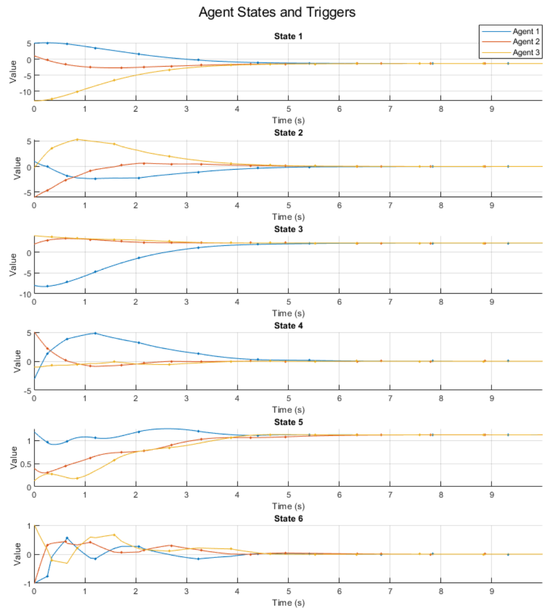

Figure 21 Gain Scheduling Scenario 1

Scenario two is successfully stabilised. As seen in Figure 22 the pitch strays to a negative angle and settles there. While the fixed linear controller could not recover the gain scheduled alternative has updated parameters which better reflect operating conditions.

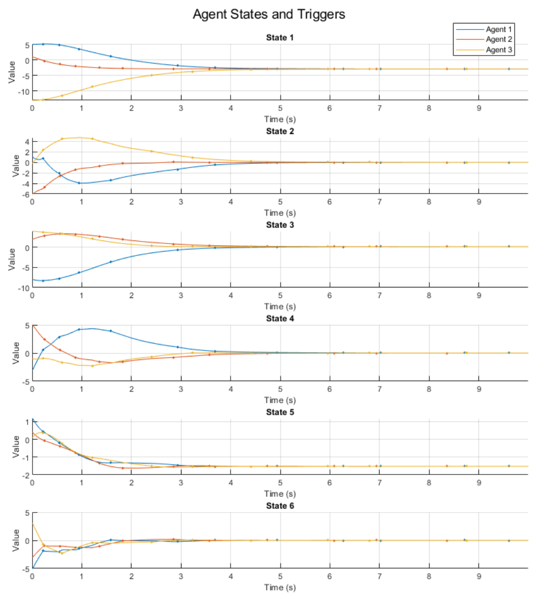

Figure 22 Gain Scheduling Scenario 2

VII. Future Work

The major deliverables remaining are finite time convergence and robustness against disturbances. These work towards the goal UAV model and better performance metrics for the sky highway use case.

Consider the network and event triggering protocol given in given in section V.B. Using the same initial conditions this is simulated again but with sensor noise and a realistic wind model. Ideally the controller should be robust and produce an analogous result. Outcomes reveal that the current approach is quite fragile.

When the measurements have a white noise power of -50dBW events excessively trigger as consensus is approached. The protocol aims to enforce perfect consensus, however the noise consistently repudiates this.

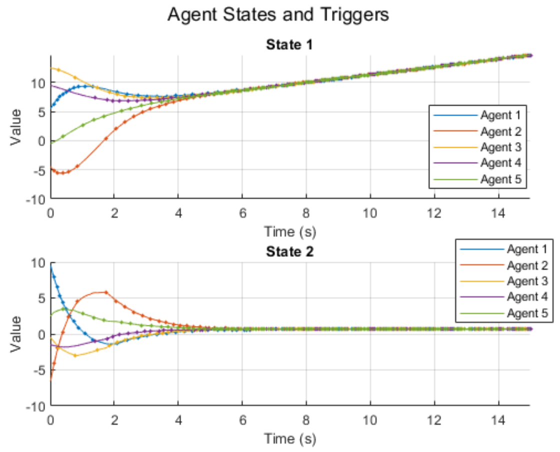

Figure 23 Scenario V.B States and Triggers with Sensor Noise

When a wind model is applied a similar effect is seen. The wind has the additional effect of becoming a virtual leader. Without having a fixed setpoint the agents are only aiming for a system average. This is regulated to the speed of the wind.

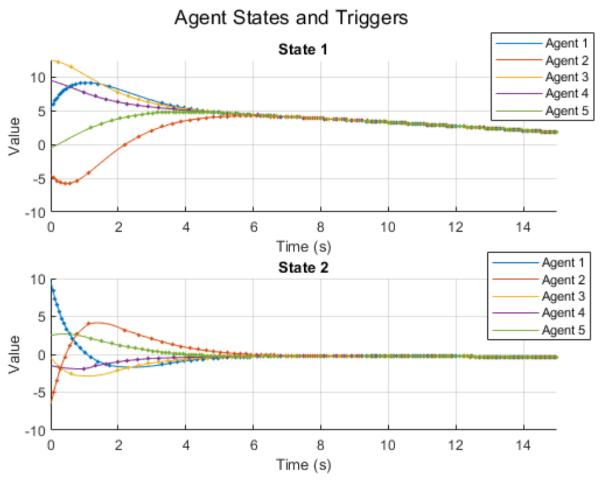

Figure 24 Scenario V.B States and Triggers with Wind Model

VIII. Conclusion

This progress report details an initial exploration into event-triggered consensus. Simulations performed for state-dependent and state-independent triggering protocols show an overall reduction in triggering instants. However, if agents do not settle at equilibrium they trigger wastefully. Using open loop estimation techniques this limitation may be overcome. This triggering method has been applied with an adaptive gain-scheduling controller to force nonlinear agents to reach consensus. Future work will drive the project towards the sky highway use case.

Appendix I[3]

A. Graph Preliminaries

A team of p vehicles may have information exchanges modelled by graphs (V_p, E_p) which are either directed or undirected. Both cases have a node set $V_p = \{1, \ldots, p\}$ and edge set $E_p \subseteq V_p \times V_p$. In the directed case edge (i, j) denotes that child node j may receive information from parent node i, although not vice versa. In the undirected case edge (i, j) signifies both nodes may receive information from one another. This may be categorised as a special directed graph case, where undirected (i, j) implies a directed couple (i, j) and (j, i). Self-edges are not allowed, unless stated. A weighted graph maps a weight to every edge.

Directed and undirected paths are sequences of edges (i_1, i_2), (i_2, i_3), … in directed and undirected graphs respectively. These are cycles instead if starting and ending at the same node.

A directed tree is where every node has a parent except for a root node, which consequentially has s directed path to its all its descendants. A directed graph is strongly connected if every node is the root of a directed tree reaching all other nodes. An undirected tree is where every pair of nodes is connected by a path. This is analogous to an undirected graph being connected.

B. Matrix Preliminaries

The adjacency matrix $\mathrm{A}_p = [\alpha_{ij}] \in \mathbb{R}^{p\times p}$of a graph reflects the weights of edges (j, i). Value a_{ij} is 0 if $(j, i) \notin E_p$, as self-edges are not allowed this causes the diagonal to be zeros. For the undirected graph the adjacency matrix is symmetrical as $(j, i) \in E_p$ requires $(i, j) \in E_p$ causing $a_{ij} = a_{ji}$. They are also balanced, meaning $\sum_{j=1}^{p} a_{ij} = \sum_{j=1}^{p} a_{ji}$ for all i.

There is a corresponding Laplacian matrix $L_p = [l_{ij}] \in \mathbb{R}^{p\times p}$ which is defined as $L_p \triangleq D_{in} - \mathrm{A}_p$. Here the in-degree matrix $D_{in} = [d_{ij}] \in \mathbb{R}^{p\times p}$ is given as $d_{ij} = 0, i \neq j$ and $d_{ii} = \sum_{j=1}^{p} a_{ij}\,, i = 1, \ldots, p$. This is not the common Laplacian matrix definition, however it has relevance to consensus algorithms.

There is also a corresponding row stochastic matrix $D_p = [d_{ij}] \in \mathbb{R}^{p\times p}$ which is nonnegative and has every row sum to one. It may be calculated as $D_p = (I + D_{in})^{-1} \cdot (I + A)$. The identity matrix $I = [i_{ij}] \in \mathbb{R}^{p\times p}$ is given as $i_{ij} = 0, i \neq j$ and $i_{ii} = 1$. D_{in} is the in-degree matrix as before. The product of these are still row stochastic. It is indecomposable and aperiodic (SIA) if $\lim_{k\to\infty} D^k = \mathbf{1}y^T$ for $y \in \mathbb{R}^n$. They have the eigenvalue 1 for eigenvector $\mathbf{1}_n$. This matrix is used to study consensus in the discrete time setting.

[3] The work in this appendix is adapted exclusively from [6].

C. Linearisation

Consider a nonlinear equation of the following form.

$$\dot{x} = f(x(t), u(t))$$

Where f is a function which maps $\boldsymbol{R}^{\boldsymbol{n}} \times \boldsymbol{R}^{\boldsymbol{m}} \to \boldsymbol{R}^{\boldsymbol{n}}$. This may be represented as a linear state space model at state $\bar{x}$ and input $\bar{u}$ operating points Jacobian matrices.

$$A = \left(\frac{\partial f}{\partial x}\right)^T |_{x=\bar{x}, u=\bar{u}} \in \boldsymbol{R}^{\boldsymbol{n\times n}}$$

$$B = \left(\frac{\partial f}{\partial u}\right)^T |_{x=\bar{x}, u=\bar{u}} \in \boldsymbol{R}^{\boldsymbol{n\times m}}$$

These can be formulated as a system model for approximate states $\tilde{x}$ and $\tilde{u}$.

$$\dot{\tilde{x}} = A\tilde{x} + B\tilde{u}$$

Appendix II

A. Testing Suite

To verify the integrity of the implementation, a suite of unit tests was developed using the inbuilt MATLAB testing framework.

Automated unit tests will be used to verify the solution correctness and coverage. These will check whether consensus is achieved using a range of total agents, initial state trajectories and network topologies. Convergence can be checked with the literature review definition, however with a sufficiently small error allowable for bounded consensus. With a limited set of numerical examples to base tests off, conclusions about novel test outcomes must be drawn from the principles reviewed.

It is impractical to verify the correct replication of a research paper via automated testing, as there is typically not exact data to compare results with. Important metrics such as the state or error over time are consistently displayed in plots rather than in a numerical form. As such, manual inspection will be required to draw conclusions.

The following table shows a preliminary list of tests. This will be expanded upon throughout the iteration process as complexity increases.

Table 2. Unit Tests

No.	**Description**	**Pass Criteria**	**Result**
A	***Automated Test Suite***		
A.1	*Agents*: 5 *Initial Values:* linear distribution *Network:* Undirected, connected	Consensus Reached	Pass
A.2	*Agents:*5 *Initial Values:* linear distribution *Network:* Undirected, disconnected	Consensus Not Reached	Pass
A.3	*Agents:* 5 *Initial Values:* exponential distribution	Consensus Reached	Pass

	Network: Undirected, connected		
A.4	*Agents:* 10 *Initial Values:* linear distribution *Network:* Undirected, connected	Consensus Reached	Pass
B	***Manual Test Suite***		
B.1	State trajectory plot	Mirrored Plot	
B.2	Transmission triggering plot	Mirrored Plot	
B.3	State error plot	Mirrored Plot	

Automated unit tests are summarised with the following results. The two succeeding figures show the network topology and state trajectories for single integrator agents.

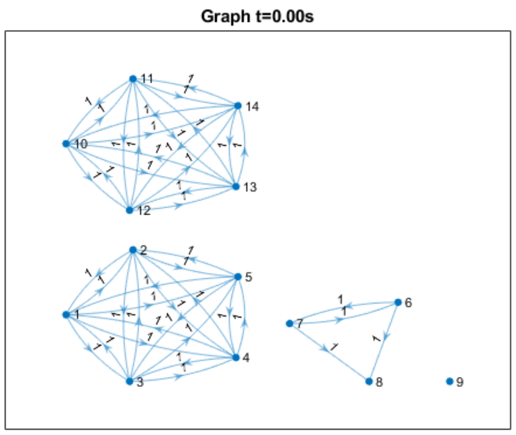

Figure 25 Test Representation Graph

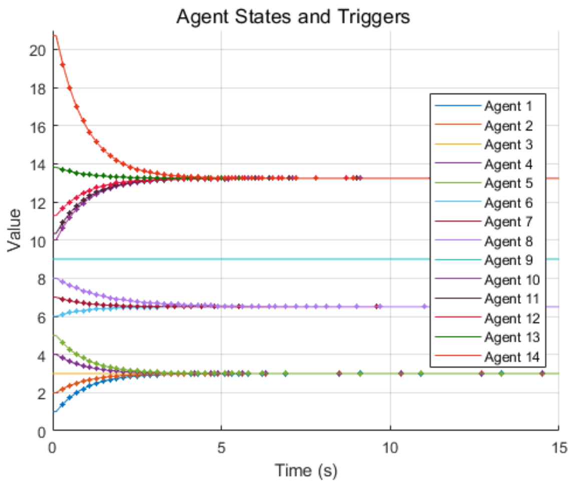

Figure 26 Test Representation States

An example manual unit test is given with succeeding figures. These show an attempted replication of first problem in [17], where related results are displayed in Fig 2. and Fig 4. A visual comparison reveals that results have similar shapes, however there is not an exact comparison. It is difficult to discern where differences stem from. The paper reports the error threshold exponent as the sampling iteration k. It is assumed this should be given as time instead to match displayed values and have consistency across different sampling periods. The network graph in Fig 1. does not match the given communications matrix. Agent three is pictured receiving from four, yet the matrix has this weighted as zero. Separate from the scenario and implementation there are likely differences in the simulation environment and algorithm. Due to ambiguities and result similarity it is assumed the replication is working as intended. It is impossible to confirm correctness.

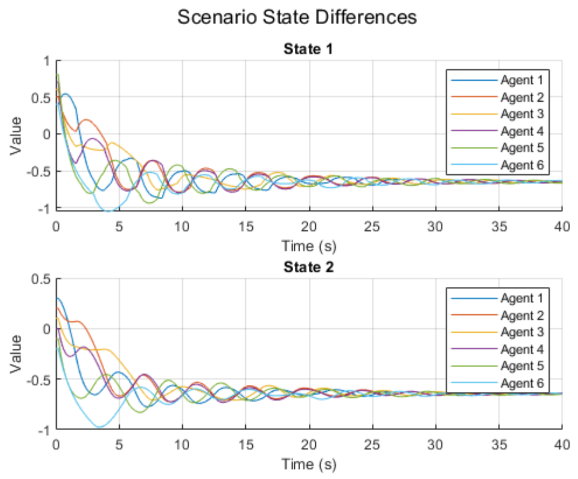

Figure 27 Toy State Trajectories

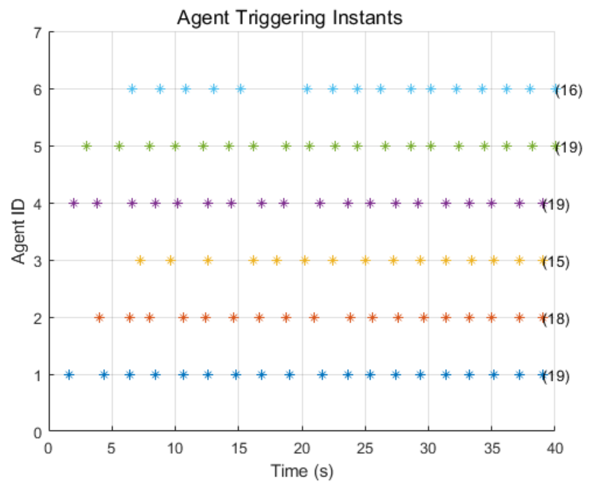

Figure 28 Toy Triggering Instants

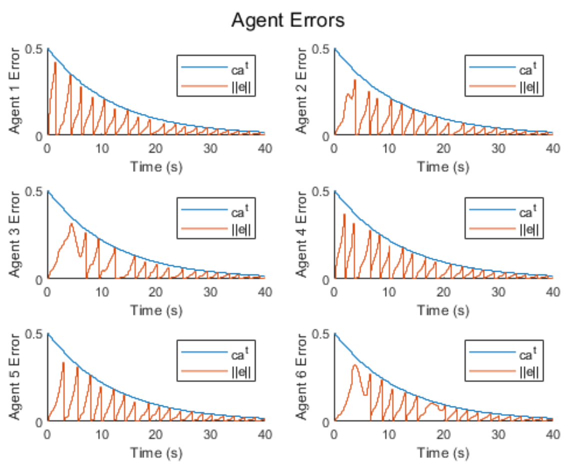

Figure 29 Toy Error Norm and Threshold

APPENDIX III

A. *Progress Summary*

The project has progressed to the development of simple event-triggered consensus control strategies. Quarter one was used to build a theory-based foundation. Quarter two was used to develop an extensible simulation environment for the initial attempts and future work. This was extended in quarter three with a simple gain scheduling nonlinear control method.

B. *Quarter 1 (Semester 2, 2020 - Project Proposal)*

This quarter the initial engineering literature review worksheet and project proposal were completed. A clear plan was established for the remainder of the investigation.

C. *Quarter 2 (Semester 2, 2020 - Progress Report)*

A strong foundation was established in this quarter to base more complex work to come. Core deliverables of continuous and discrete time consensus were complete. Initial event-triggered and model-based event-triggered protocols were built on this. An advance on phase two started where switching topologies, sensor noise and transmission delays were modelled. The empirical learnings not gleamed from the quarter one theory have been added to the literature review.

The MATLAB simulation environment was written with an object-oriented approach to facilitate the iterative nature of this project. Core concepts such as inheritance and abstraction ensure that modifications and extensions are simple.

D. *Quarter 3 (Semester 1, 2021 - Progress Report)*

This quarter has focussed on the development of nonlinear control techniques. A few have been investigated/attempted but with limited success. A simple gain scheduled control was successfully implemented. The project focus has been narrowed to focus on the rejection of disturbances.

E. *Quarter 4 (Semester 1, 2021 – Final Report)*

N/A

F. *Design Regime*

A high-level process flow displaying tasks and interdependencies for both phases is pictured The succeeding figure. This is broken down into a Gantt chart projected timeline, documented within Appendix III.G.

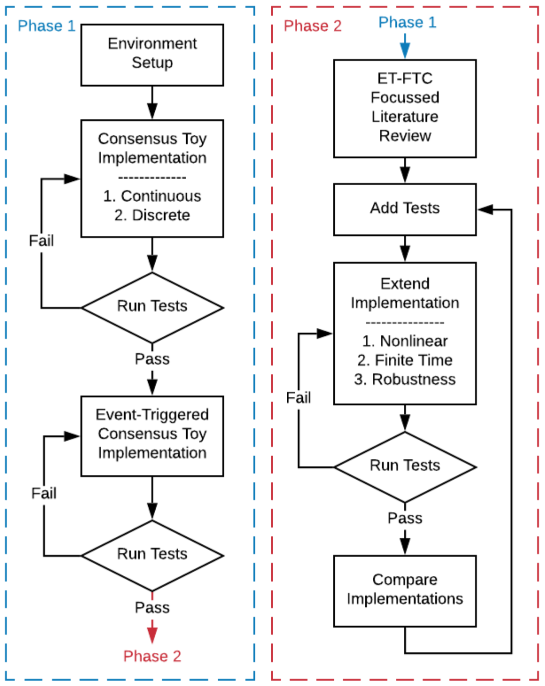

Figure 30 Project Workflow

G. Project Timeline

PHASE 1. Quarters 1, 2 Reflection (7 Nov 2020)

The updated Gantt timeline is shown as follows. The main change is the additional of subtask 1.4 Modelling Imperfections. Some minor changes have been made to subtask 1.3 Event-Triggered Implementation to better reflect the process.

I am happy with the first phase progress. The initial project proposal planned for phase one to model an event triggered protocol for single integrator agents under a strongly connected time invariant topology. These deliverables were finished and extended. There have been several approaches explored which model double integrator agents under switching topologies. The case for phase two importance has been made by modelling imperfections and observing the detriments. I have a positive outlook for successful completion and strong outcomes. There is still plenty of work to do and the triggering strategy will be replaced. The technical learnings and observations from phase one will be invaluable for this.

A nontechnical takeaway is that the exact replication of research papers is very difficult. This follows the trend given in Appendix II. Numerical examples do not always detail all the specifics and required values. Simulation algorithms are rarely given and very high level; small changes such as whether agents broadcast on start-up have a butterfly effect to completely change the outcome. Subtask 1.3.6 Testing and Refinement took much longer than anticipated for these reasons. To improve on this in future desired preciseness of replication will be relaxed. The timeline for the next phase has been altered to expand the initial literature review and shrink development time so the final strategy is understood deeply and the refinement will be brief. The first pass at implementation can be feasibly done in a brief period due to the code base extensibility.

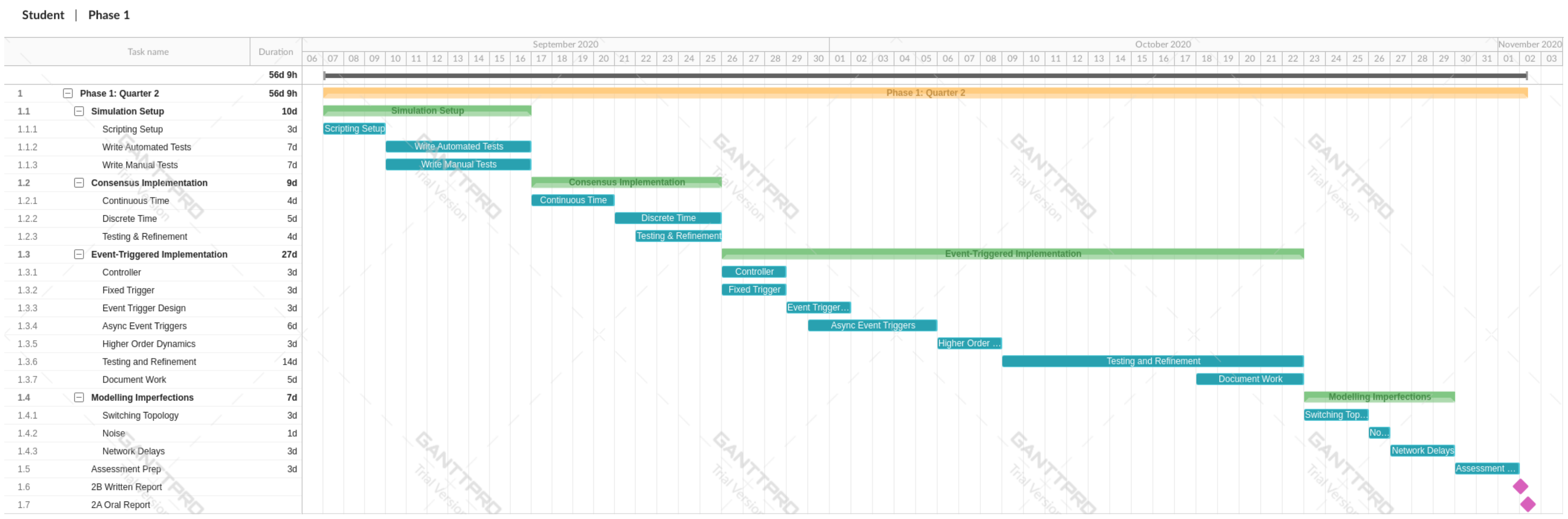

	Task name	Duration
		56d 9h
1	Phase 1: Quarter 2	56d 9h
1.1	Simulation Setup	10d
1.1.1	Scripting Setup	3d
1.1.2	Write Automated Tests	7d
1.1.3	Write Manual Tests	7d
1.2	Consensus Implementation	9d
1.2.1	Continuous Time	4d
1.2.2	Discrete Time	5d
1.2.3	Testing & Refinement	4d
1.3	Event-Triggered Implementation	27d
1.3.1	Controller	3d
1.3.2	Fixed Trigger	3d
1.3.3	Event Trigger Design	3d
1.3.4	Async Event Triggers	6d
1.3.5	Higher Order Dynamics	3d
1.3.6	Testing and Refinement	14d
1.3.7	Document Work	5d
1.4	Modelling Imperfections	7d
1.4.1	Switching Topology	3d
1.4.2	Noise	1d
1.4.3	Network Delays	3d
1.5	Assessment Prep	3d
1.6	2B Written Report	
1.7	2A Oral Report	

Figure 31 Gantt Chart Remainder Phase 1

PHASE 2. Quarter 3 Reflection (25 April 2021)

The Gantt chart for progress, and attempted works is shown throughout the semester. Coordinate transformations, sliding mode control and multiple-input multiple-output finite time convergence were each investigated and trialled, but with limited success. Struggles have been caused by lack of foundational knowledge required for some of the complicated mathematical concepts.

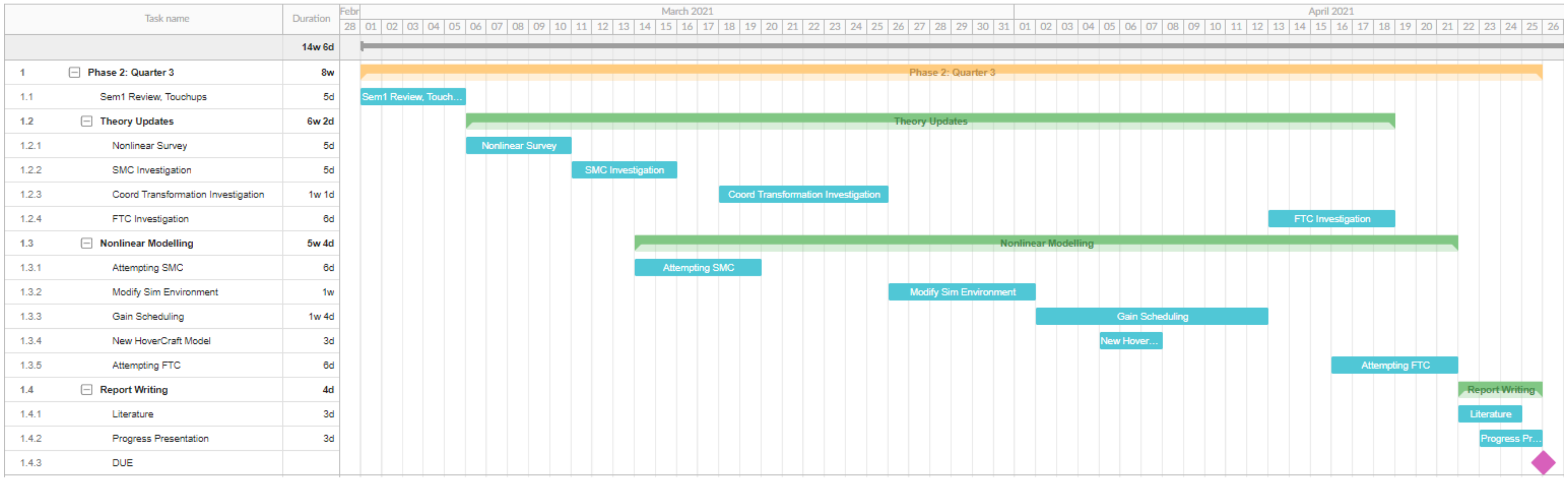

	Task name	Duration
		14w 6d
1	Phase 2: Quarter 3	8w
1.1	Sem1 Review, Touchups	5d
1.2	Theory Updates	6w 2d
1.2.1	Nonlinear Survey	5d
1.2.2	SMC Investigation	5d
1.2.3	Coord Transformation Investigation	1w 1d
1.2.4	FTC Investigation	6d
1.3	Nonlinear Modelling	5w 4d
1.3.1	Attempting SMC	6d
1.3.2	Modify Sim Environment	1w
1.3.3	Gain Scheduling	1w 4d
1.3.4	New HoverCraft Model	3d
1.3.5	Attempting FTC	6d
1.4	Report Writing	4d
1.4.1	Literature	3d
1.4.2	Progress Presentation	3d
1.4.3	DUE	

Figure 32 Gantt Chart Projected Phase 2 Quarter 3

PHASE 2. Quarter 4 Plan (25 April 2021)

Seven weeks remain to complete the project. Within this time the controller needs provide finite time convergence, and robustness against disturbances. There are three avenues which are most likely to solve this problem. For a successful finish a singular one needs to be focussed on. These are listed in order of preference as follows. Ranks are decide with perceived ease of implementation and effectiveness towards the design objective.

1. Event-triggered sliding mode control
2. A multi-input multi-output linear finite time control strategy with gain scheduling and disturbance observer
3. A multi-input multi-output nonlinear finite time control strategy coupled with disturbance observer

The biggest prohibiting factor against completing these will be the theoretical understanding. To remedy this concern half of phase four time will be dedicated to a written literature review. In contrast quarter three was mostly reading, and only gave a high level of understanding. This action should facilitate the design stages for the contextualisation within the UAM project scope. The actual coding implementation should be brief, especially as the simulation framework is quite mature and robust. With a few options for completing the project, there are a couple of potential timelines.

Timeline A: This timeline ends with a successful event-triggered sliding mode control implementation. The first week is dedicated to a written literature survey. With sliding mode being a widely studied regime there is plenty to cover. When combined with even-triggering there is even more. If at the end of this first week understanding and confidence are built then this timeline will continue. A basic implementation follows. Succeeding this advanced research on algorithms to increase performance and reduce sliding mode chattering will be studied. This concludes the final solution research stage, and synchronises with project Timeline B.

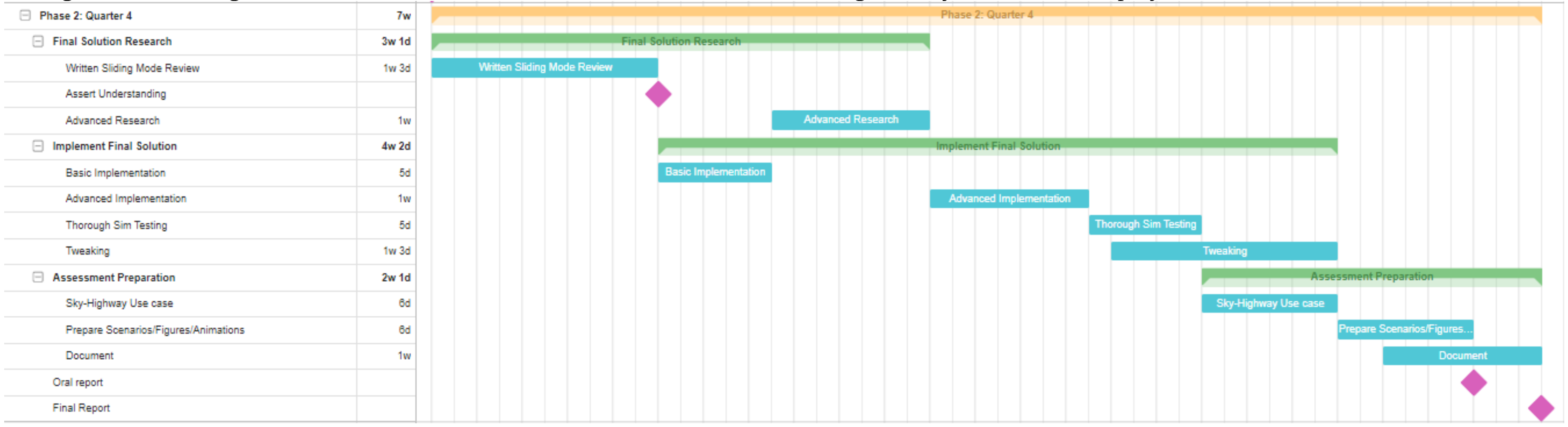

Phase 2: Quarter 4	7w
Final Solution Research	3w 1d
Written Sliding Mode Review	1w 3d
Assert Understanding	
Advanced Research	1w
Implement Final Solution	4w 2d
Basic Implementation	5d
Advanced Implementation	1w
Thorough Sim Testing	5d
Tweaking	1w 3d
Assessment Preparation	2w 1d
Sky-Highway Use case	6d
Prepare Scenarios/Figures/Animations	6d
Document	1w
Oral report	
Final Report	

Figure 33 Gantt Chart Projected Phase 2 Quarter 4 (Timeline A)

Timeline B: This timeline will be shifted to if sliding mode confidence and understanding are not sufficiently developed. It ends with implementation of either avenue two or three which is loosely based on a finite-time input control function and disturbance rejection through an observer. Two more written review periods are enforced at the beginning of this timeline to ensure that the concepts are solidified.

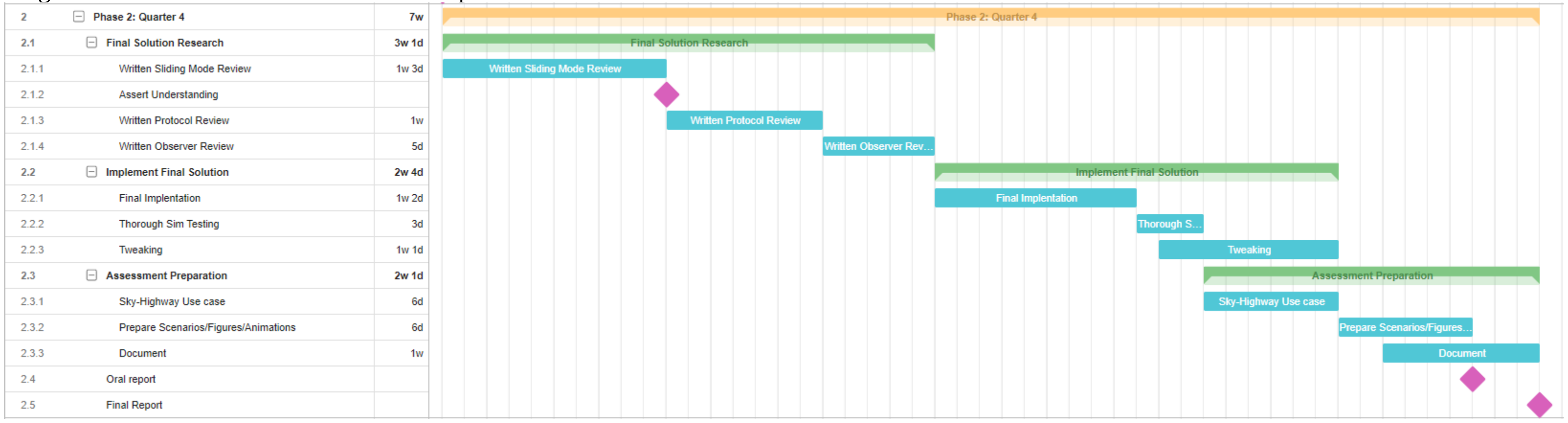

2	Phase 2: Quarter 4	7w
2.1	Final Solution Research	3w 1d
2.1.1	Written Sliding Mode Review	1w 3d
2.1.2	Assert Understanding	
2.1.3	Written Protocol Review	1w
2.1.4	Written Observer Review	5d
2.2	Implement Final Solution	2w 4d
2.2.1	Final Implentation	1w 2d
2.2.2	Thorough Sim Testing	3d
2.2.3	Tweaking	1w 1d
2.3	Assessment Preparation	2w 1d
2.3.1	Sky-Highway Use case	6d
2.3.2	Prepare Scenarios/Figures/Animations	6d
2.3.3	Document	1w
2.4	Oral report	
2.5	Final Report	

Figure 34 Gantt Chart Projected Phase 2 Quarter 4 (Timeline B)

Succeeding either Timeline A or Timeline B the main concepts required for the final implementation should be clear. The final implementation is then developed and tested. In parallel with tweaks the sky-highway use case is extended with the final implementation. This is all the necessary preparation before resources are collated for assessment.

Appendix IV

This appendix highlights the brief exploration into sliding mode control so far. It is not intended as a comprehensive review. It is a placeholder before this work is expanded and added to the main report body. Contents are adapted from [32]

A. Literature

{ This is to be added as section II.F.2}

Sliding mode control is a non-linear technique which provides robustness, reduced order dynamics and finite-time convergence. Based on the current state space position it applies a discontinuous control signal which forces systems to slide along a manifold s. This makes it a variable structure system.

The primary limitation of sliding mode control is chattering. This refers to high-frequency oscillations with a finite amplitude. It is undesirable as it can excite unmodelled dynamics and cause actuator wear degradation. It also counteracts the drivers for event-triggered control.

B. Initial Testing

{ This is to be added as section VI.C}

Consider a single agent with the following dynamics.

$$\begin{bmatrix}\dot{x}_1\\ \dot{x}_2\end{bmatrix} = \begin{bmatrix}0 & 1\\ 0 & 0\end{bmatrix}\begin{bmatrix}x_1\\ x_2\end{bmatrix} + \begin{bmatrix}0\\ 1\end{bmatrix}u$$

A state feedback controller is designed with gains as

$$u = -[2 \quad 5]x$$

A mode controller is designed as

$$s = [1.5 \quad 1]x$$

$$u = -1.5x_2 - 1.5sign(s)$$

The following two figures compares these two controllers. The state feedback controller converges asymptotically, whereas the sliding mode controller does so in finite time. The latter suffers from a fast switching frequency.

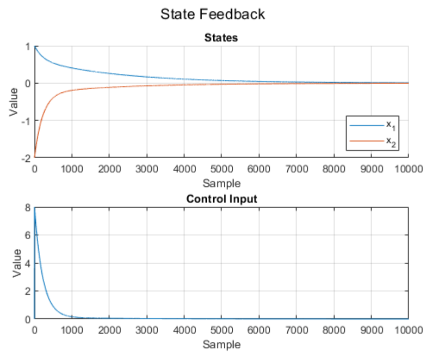

Figure 35 State Feedback Example

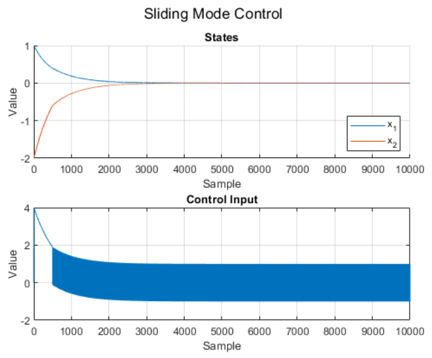

Figure 36 Sliding Mode Example

Consider the addition of bounded noise which alters the dynamics as follows.

$$\begin{bmatrix}\dot{x}_1\\ \dot{x}_2\end{bmatrix} = \begin{bmatrix}0 & 1\\ 0 & 0\end{bmatrix}\begin{bmatrix}x_1\\ x_2\end{bmatrix} + \begin{bmatrix}0\\ 1\end{bmatrix}(u + \sin(2t))$$

This noise is tested with the previously designed controllers. Results are pictured in the succeeding tow figures. The state feedback does not provide cancellation, whereas sliding mode does.

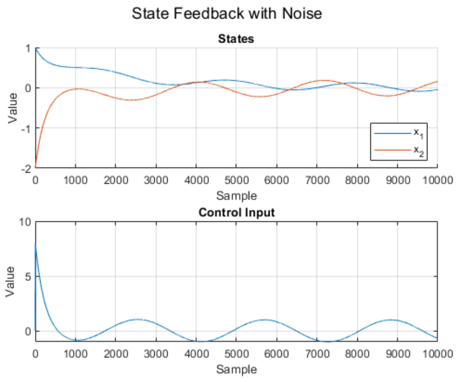

Figure 37 State Feedback Example with Noise

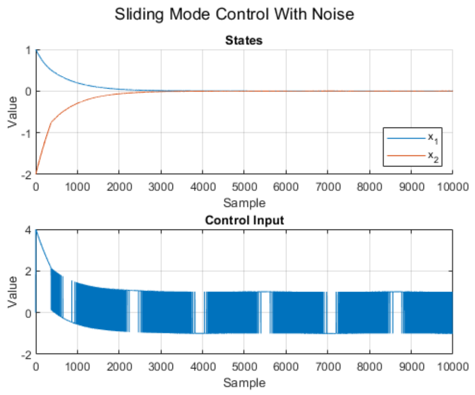

Figure 38 Sliding Mode Example with Noise

References

[1] A. Straubinger, R. Rothfeld, M. Shamiyeh, K.-D. Buechter, J. Kaiser and K. O. Ploetner, “An overview of current research and developments in urban air mobility – Setting the scene for UAM introduction,” *Journal of Air Transport Management,* vol. 87, 2020.

[2] V. Bulusu, “Urban Air Mobility: Deconstructing the Next Revolution in Urban Transportation - Feasibility, Capacity and Productivity,” ProQuest LLC, Ann Arbor, 2019.

[3] Uber Elevate, "Fast forwarding to the future of on-demand, urban aviation," Uber Technologies Inc, 2020. [Online]. Available: https://www.uber.com/in/en/elevate/uberair/. [Accessed 30 August 2020].

[4] Airbus, “Urban Air Mobility – the sky is yours,” Airbus Group, 27 November 2018. [Online]. Available: https://www.airbus.com/newsroom/stories/urban-air-mobility-the-sky-is-yours.html. [Accessed 30 August 2020].

[5] X. Yang and P. Wei, “Scalable Multi-Agent Computational Guidance with Separation Assurance for Autonomous Urban Air Mobility,” *American Institute of Aeronautics and Astronautics,* vol. 43, no. 8, pp. 1473-1486, 2020.

[6] W. Ren and R. W. Beard, Distributed Consensus in Multi-vehicle Cooperative Control, London: Springer, 2008.

[7] A. Bemporad, M. Heemels and M. Johansson, Networked Control Systems, Berlin: Springer, 2010.

[8] X. Wang and M. D. Lemmon, “Event-Triggering in Distributed Networked Control Systems,” *IEEE Transactions on Automatic Control,* vol. 56, no. 3, pp. 586-601, 2011.

[9] L. Ding, Q.-L. Han, X. Ge and X.-M. Zhang, “An Overview of Recent Advances in Event-Triggered Consensus of Multiagent Systems,” *IEEE Transactions on Cybernetics,* vol. 48, no. 4, pp. 1110-1123, 2018.

[10] K. L. Moore, M. D. Weiss, J. P. Steele, C. Meehan, J. Hulbert, E. Larson and A. Weinstein, “Experiments with autonomous mobile radios for wireless tethering in tunnels,” *Journal of Defense Modeling and Simulation,* vol. I, no. 9, p. 45–58, 2012.

[11] X. Ge, Q.-L. Han, D. Ding, X.-M. Zhang and B. Ning, “A survey on recent advances in distributed sampled-data cooperative,” *Neurocomputing,* vol. 275, pp. 1684-1701, 2018.

[12] Z. Zhang, F. Hao, L. Zhang and L. Wang, “Consensus of linear multi-agent systems via event-triggered control,” *International Journal of Control,* vol. 87, no. 6, pp. 1243-1251, 2014.

[13] S. S. Kia, J. Cortes and S. Martinez, “Distributed event-triggered communication for dynamic average,” *Automatica,* vol. 59, pp. 112-119, 2015.

[14] G. S. Seyboth, D. V. Dimarogonas and K. H. Johansson, “Event-based broadcasting for multi-agent average consensus,” *Automatica,* vol. 49, no. I, pp. 245-252, 2012.

[15] E. Garcia, P. J. Antsaklis and L. A. Montestruque, Model-Based Control of Networked Systems, New York: Springer International Publishing , 2014.

[16] Y. Liu and X. Hou, “Event-triggered consensus control of disturbed multi-agent systems using output feedback,” *ISA Transactions,* vol. 91, pp. 166-173, 2019.

[17] D. Yang, X. Liu and W. Chen, “Periodic event/self-triggered consensus for general continuous-time linear multi-agent systems under general directed graphs,” *IET Control Theory and Applications,* vol. 9, no. 3, p. 428–440, 2015.

[18] Y. W. Meng, L. Xie and R. Lua, “An input-based triggering approach to leader-following problems; Hongye Su; Zheng-Guang Wu,” *Automatica,* vol. 75, p. 221–228, 2017.

[19] V. T. Haimo, “Finite Time Controllers,” *SIAM Journal on Control and Optimization,* vol. 24, no. 4, pp. 760-770, 1986.

[20] J. Lui, Y. Yu, H. He and C. Sun, “Team-Triggered Practical Fixed-Time Consensus of Double-Integrator Agents With Uncertain Disturbance,” *IEEE Transactions on Cybernetics,* vol. Early Access, pp. 1-10, 2020.

[21] X. Lu, “Distributed Event-Triggered Control for Prescribed Finite-Time Consensus of Linear Multi-Agent Systems,” *IEEE Access,* vol. 8, pp. 129146 - 129152, 2020.

[22] C. Du, X. Liu, W. Ren, P. Lu and H. Liu, “Finite-Time Consensus for Linear Multiagent Systems via Event-Triggered Strategy Without Continuous Communication,” *IEEE Transactions on Control of Network Systems,* vol. 7, no. 1, pp. 19-29, 2020.

[23] J. Liu, Y. Zhang, Y. Yu and C. Sun, “Fixed-Time Event-Triggered Consensus for Nonlinear Multiagent Systems Without Continuous Communications,” *IEEE Transactions on Systems, Man, and Cybernetics: Systems,* vol. 49, no. 11, pp. 2221-2229, 2018.

[24] Q. Lu, Q.-L. Han, B. Zhang, D. Liu and S. Liu, “Cooperative Control of Mobile Sensor Networks for Environmental Monitoring: An Event-Triggered Finite-Time Control Scheme,” *IEEE Transactions on Cybernetics,* vol. 47, no. 12, pp. 4134-4147, 2017.

[25] W. J. R. J. S. Shamma, “Research on gain scheduling,” *Automatica,* vol. 36, pp. 1401-1425, 2000.

[26] P. Swarnkar, S. K. Jain and R. Nema, “Adaptive Control Schemes for Improving the Control System Dynamics: A Review,” *IETE Technical Review,* vol. 31, no. 1, pp. 17-33, 2014.

[27] T. Perez, “Modelling of Physical Dynamical Systems,” Queensland University of Technology, Brisbane, 2017.

[28] Z. Jin, S. Waydo, E. B. Wildanger, M. Lammers, H. Scholze, P. Foley, D. Held and R. M. Murray, “MVWT-II: the second generation Caltech Multi-Vehicle Wireless Testbed,” in *Proceedings of the 2004 American Control Conference*, Boston, 2004.

[29] A. Battista and D. Ni, “A Comparison of Traffic Organization Methods for Small Unmanned Aircraft Systems,” *Transportation Research Record,* vol. 2672, pp. 21-30, 2018.

[30] MathWorks, “atmoshwm,” 2021. [Online]. Available: https://www.mathworks.com/help/aerotbx/ug/atmoshwm.html. [Accessed 8 April 2021].

[31] P. Sachs, “Introduction,” in *Wind Forces in Engineering,* Guildford, Biddles Ltd, 1978, pp. 1-8.

[32] Y. Shtessel, C. Edwards, L. Fridman and A. Levant, Sliding Mode Control and Observation, New York: Birkhäuser, 2014.

[33] P. Tabuada, “Event-Triggered Real-Time Scheduling of Stabilizing Control Tasks,” *IEEE Transactions on Automatic Control,* vol. 52, no. 9, pp. 1680-1685, 2007.

[34] D. Liuzza, D. V. Dimarogonas, M. d. Bernardo and K. H. Johanssona, “Distributed model based event-triggered control for synchronization of multi-agent systems,” *Automatica,* no. 73, pp. 1-7, 2016.